Biochimica et Biophysica Acta 1842 (2014) 2136–2146

Contents lists available at ScienceDirect

Biochimica et Biophysica Acta

journal homepage: www.elsevier.com/locate/bbadis

Oligomerization of Cysteine String Protein alpha mutants causing adult neuronal ceroid lipofuscinosis

Yong-quan Zhang [a,*], Sreeganga S. Chandra [a,b,**]

[a] Program for Cellular Neuroscience, Neurodegeneration and Repair, Department of Neurology, Yale School of Medicine, New Haven, CT 06536, USA
[b] Department of Molecular, Cellular and Developmental Biology, Yale University, New Haven, CT 06536, USA

ARTICLE INFO

Article history:
Received 17 March 2014
Received in revised form 20 June 2014
Accepted 16 July 2014
Available online 23 July 2014

Keywords:
ATPase
Heat shock cognate, J domain
Lysosomal storage disease
Synapse maintenance

ABSTRACT

Cysteine String Protein alpha (CSPα) is a palmitoylated, synaptic vesicle co-chaperone that is essential for neuroprotection. Two mutations in CSPα — L115R and L116Δ — cause adult neuronal ceroid lipofuscinosis (ANCL), a dominantly-inherited neurodegenerative disease. To elucidate the pathogenesis of ANCL, the intrinsic biochemical properties of human wildtype (WT) and disease mutant CSPα were examined. Mutant proteins purified from *Escherichia coli* exhibited high potency to oligomerize in a concentration, temperature, and time dependent manner, with L115R possessing the greatest potency. When freshly purified, ANCL mutant proteins displayed normal co-chaperone activity and substrate recognition similar to WT. However, co-chaperone activity was impaired for both CSPα mutants upon oligomerization. When WT and mutant CSPα were mixed together they co-oligomerized leading to an overall decrease of co-chaperone activity. The oligomerization properties of ANCL mutants were faithfully replicated in HEK 293T cells. Interestingly, the oligomers were covalently tagged by ubiquitination instead of palmitoylation. Taken together, ANCL mutations result in both a gain and partial loss-of-function.

1. Introduction

Neuronal ceroid lipofuscinoses (NCLs) are inherited, progressive neurodegenerative diseases that occur mainly in children, and on occasion, also in adults. They are characterized clinically by gait abnormalities, seizures, and dementia. Morphologically, NCLs are identified by the lysosomal accumulation of autofluorescent storage material (lipofuscin) and the loss of neurons, predominantly in the cortex and cerebellum [1–3]. To date, mutations in 14 genes have been identified to cause NCLs [4]. All, but one, *CLN4*/*DNAJC5* encoding a mutant Cysteine String Protein alpha (CSPα), are familially inherited in an autosomal recessive manner. While the disruption of normal protein function by nonsense or missense mutations has been demonstrated to underlie the pathogenesis of autosomal recessive NCL, little has been known about the unique autosomal dominant form of NCL (*CLN4*) [5,6].

CSPα is a co-chaperone enriched in the presynaptic terminal. It is highly conserved among mammals [7] (Fig. 1). CSPα has 3 domains—an N-terminal J-domain, the middle cysteine string domain which is palmitoylated on 14 cysteines, and a C-terminal substrate binding domain (Fig. 1A). CSPα forms a chaperone complex with Hsc70 and the tetratricopeptide protein SGT, and plays a crucial role in synapse maintenance by acting on select substrates [7–9]. These include SNAP-25 and dynamin 1, which are essential for synaptic vesicle recycling [10–12]. The two mutations (L115R and L116Δ) that cause ANCL are in the cysteine string domain [13–15] (Fig. 1B). As the name indicates ANCL is a late-onset, dominant form of NCL.

Little is known about the pathogenesis of ANCL. The previous molecular study on ANCL suggests that the two L115R and L116Δ mutations interfere with palmitoylation of CSPα [16]. Even so, ANCL CSPα mutants were shown to aggregate in a palmitoylation dependent manner when heterologously overexpressed with palmitoyltransferases [16]. This raises the question of how the ANCL mutant proteins intrinsically behave. In this study, we purified WT and ANCL mutant CSPα proteins from *Escherichia coli* and systemically examined their co-chaperone activity, dynamics of oligomerization, and subsequently confirmed these findings in mammalian cell lines. Remarkably, our results show that oligomerization of mutant CSPα can occur even in the absence of palmitoylation and leads to a loss-of-co-chaperone function.

* Correspondence to: Y.-G Zhang, 295 Congress Ave, BCMM 149, New Haven, CT 06536, USA. Tel.: +1 203 785 4741; fax: +1 203 737 2267.
** Correspondence to: S. S. Chandra, 295 Congress Ave, BCMM 154D, New Haven, CT 06536, USA. Tel.: +1 203 785 6172; fax: +1 203 737 2267.
E-mail addresses: yongquan.zhang@yale.edu (Y. Zhang), sreeganga.chandra@yale.edu (S.S. Chandra).

http://dx.doi.org/10.1016/j.bbadis.2014.07.009
0925-4439/

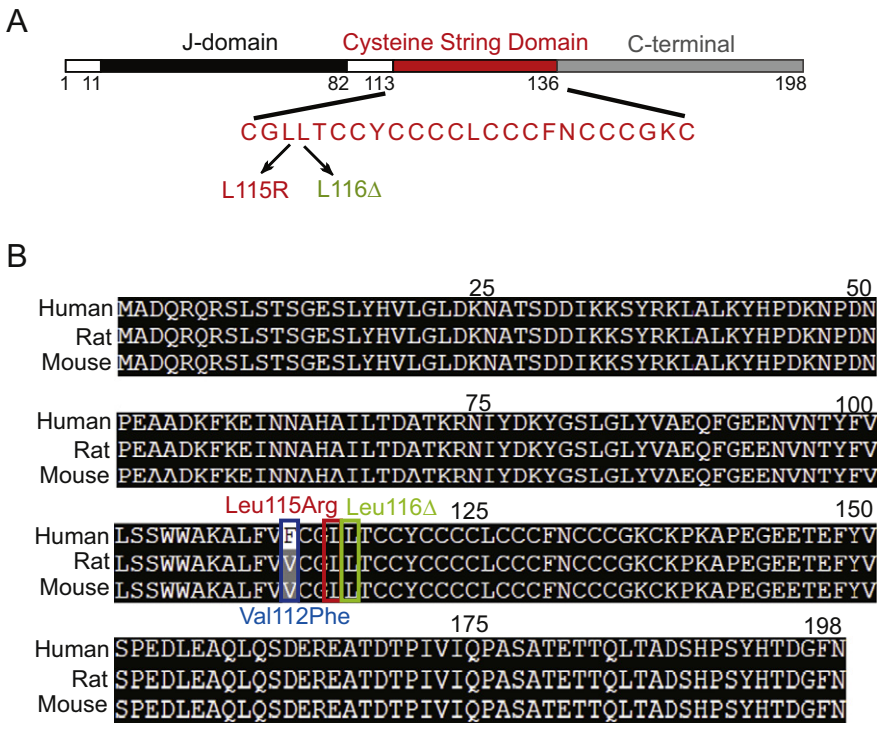

Fig. 1. Position of ANCL mutations in CSPα. (A) The domain organization and position of ANCL mutations in human CSPα protein. The numbers define the amino acids that border the different domains. Amino acid sequence of the Cysteine String Domain is illustrated in detail and the two mutations L115R and L116Δ are indicated by arrows. (B) Alignment of human, rat, and mouse CSPα protein sequences. Consensus amino acids are marked by black highlights and variable amino acids are indicated by gray and white. The boxes show the site of ANCL mutant human CSPα and the one difference between the human and mouse sequences.

2. Materials and methods

2.1. Animals

All mice are kept according to an IACUC approved protocol in a YARC mouse colony.

2.2. Materials

Adenosine 5′-diphosphatesodium salt (ADP-Na), adenosine 5′-triphosphatesodium salt (ATP-Na), 50% hydroxylamine (HA) solution, and urea were purchased from Sigma. Pfu Turbo DNA polymerase was purchased from Agilent Technologies. Thrombin was obtained from GE Healthcare. GenePORTER® 3000 Transfection Reagent was purchased from Genlantis, while Ni-NTA Agarose was obtained from QIAGEN. The following primary antibodies were used at the indicated concentration: CSPα (rabbit, 1:50, Chemicon AB1576), CSPα C terminus (rabbit, 1:6000, Enzo ADI-VAP-SV003-E), CSPα N terminus (goat, 1:200, Santa Cruz, N-17), SGT (rabbit, 1:1000, CHAT33), dynamin 1 (rabbit, 1:1000, Epitomics EP801Y), SNAP-25 (mouse, 1:20,000, Sternberger Monoclonals Inc. SMI-81), α-synuclein (rabbit, 1:1000, T2270), ubiquitin (mouse, 1:1000, LifeSensor, FK2), FLAG (rabbit, 1:1000, Sigma, F7425), and Myc (Mouse, 1:1000, Thermo Scientific, A7).

2.3. Site-directed mutagenesis

Site-directed mutagenesis was performed using QuickChangeTM Site-directed Mutagenesis kit (Stratagene). The primers for the mutagenesis were as follows:

Rat CSPα cDNA to cDNA encoding human CSPα;
Sense: 5′-CAAGGCGCTGTTCGTC(*G*/T)TCTGTGGCCTCCTCAC;
Antisense: GTGAGGAGGCCACAGA(*C*/A)*GACGAACAGCGCCTTG*;

L115R mutation:
Sense: 5′-TTCGTCTTCTGTGGCC(*T*/G)CCTCACCTGCTGCTAC;
Antisense: 5′-GTAGCAGCAGGTGAGG(*A*/C)GGCCACAGAAGACGAA.
L116Δ mutation:
Sense: -TCGTCTTCTGTGGCCTC(*CTC*/Δ)ACCTGCTGCTACTGCTG;
Antisense: 5′-CAGCAGTAGCAGCAGGT(*GAG*/Δ)GAGGCCACAGAAGACGA.
For insertion of stop codon TAA downstream base pair 408 to delete 'C' terminus of CSPα:
Sense: 5′-CTGCTGTGGGAAGTGC(TAA)AAGCCCAAGGCACCTG.
Antisense: 5′-CAGGTGCCTTGGGCTT(TTA)GCACTTCCCACAGCAG.

The italic letters in brackets indicate the original nucleotides. The amplified mutant plasmids were confirmed by sequencing.

2.4. Construction of plasmids

All site-directed mutagenesis were performed on CSPα sequences subcloned into either PGEX-KG or lentiviral expression plasmids. To insert Myc or FLAG tags upstream of CSPα in lentiviral expression plasmids, XbaI was used to excise the vector and ligated with the annealed oligonucleotides encoding Myc or FLAG. The start codon ATG of CSPα was then removed by site-directed mutagenesis as above. The inserted oligonucleotides are as follows:

Myc: Sense 5′-CTAGAATGGAACAAAAACTTATTTCTGAAGAAGATCTG;
Antisense 5′-CTAGCAGATCTTCTTCAGAAATAAGTTTTTGTTCCATT;
FLAG: Sense 5′-CTAGAATGGATTACAAGGATGACGATGACAAG;
Antisense 5′-CTAGCTTGTCATCGTCATCCTTGTAATCCATT.
The primers for site-directed mutagenesis are as follows:
Myc-CSPα ATG deletion:

Sense: 5′-GAAGATCTGCTAGAC(*ATG*/Δ)GCTGACCAGAGGCAG;
Antisense: 5′-CTGCCTCTGGTCAGC(*CAT*/Δ)GTCTAGCAGATCTTC.
FLAG- CSPα ATG deletion:
Sense: 5′-CGATGACAAGCTAGAC(*ATG*/Δ)GCTGACCAGAGGCAGC;
Antisense: 5′-GCTGCCTCTGGTCAGC(*CAT*/Δ)GTCTAGCTTGTCATCG.

To generate the J domain deletion CSPα construct an XbaI restriction site with an additional a nucleotide C was inserted downstream base pair 246 of CSPα PGEX-KG plasmid by site-directed mutagenesis. The J domain fragment was excised out by XbaI digestion and the final CSPα construct without the J domain was obtained by a subsequent re-ligation. The primers for site-directed mutagenesis are as follows:

Sense: 5′-CAAGTATGGCTCGCTG(TCTAGAC)GGGCTCTATGTGGCTG;
Antisense: 5′-CAGCCACATAGAGCCC(GTCTAGA)CAGCGAGCCATACTTG.

All clones were confirmed by sequencing.

2.5. Protein purification

GST-Hsc70, GST-WT, and mutant GST-CSPα were expressed in BL21(DE3) *E. Coli* and purified as previously described [12]. GST tags were cleaved with thrombin and removed by affinity chromatography. His tagged SGT was purified using Ni-NTA agarose beads based on the description in the manual (QIAGEN). To prevent disulfide bond formation, 2 mM TCEP or DTT was added to the purified proteins. The concentration of the protein preparations was obtained spectrophotometrically. Purified protein was aliquoted and stored at −80 °C before use.

2.6. Immunoblotting

Equal amounts for purified protein were loaded for SDS-PAGE, while for HEK 293 T cell lysates equal volumes were loaded. The proteins were probed first with specific primary antibodies and then with IRDye conjugated secondary antibodies. Protein bands were quantified on a LI-COR Odyssey infrared imaging system. All CSPα bands over 53 kDa were selected and quantified as HMW oligomers.

2.7. ATPase assay

ATPase activity was assayed using a colorimetric approach as described by Chamberlain and Burgoyne [17]. Prior to the start of the ATPase assay, 40 μM of purified WT and mutant CSPα (or a mixture of 20 μM of each) was pre-warmed for 1 min or for 24 h at 37 °C. Purified protein (1 μmol) was incubated in ATPase assay buffer (10 mM $MgCl_2$, 5 mM KCl, 50 mM Tris, pH 7.5) for 5 min, followed by addition of 1 mM ATP to start the reaction. Aliquots (10 μL) of the reaction were withdrawn every 4 min and incubated with 800 μL of MG solution (0.034% malachite green, 1.04% NH_4-molybdate, 1 M HCl, 0.04% Tween-20) for 1 min and quenched with 100 μL of 34% Na-citrate. OD_{650} was measured 5 min after quenching. The experiment was calibrated using 1 mM KH_2PO_4 and the concentration of free phosphate was calculated based on the equation $1OD_{650} = 9.45$ nmol Pi.

2.8. GST pull-down

WT or ANCL mutant GST-CSPα fusion proteins were purified from *E. coli* as described [12]. Fusion protein bound to beads was mixed with brain extract (in 20 mM HEPES, pH 7.4, 100 mM NaCl, 1% Triton X-100) and incubated for at least 4 h by rotating at 4 °C. Depending on experimental condition, 5 mM ADP or ATP was added to the mixture as noted. The beads were then washed 3 times for 10 min with HEPES buffer containing 1% Triton X-100 and finally eluted with SDS-PAGE sample buffer by boiling for 10 min.

2.9. Immunoprecipitation

HEK 293T cells expressing WT or mutant CSPα were lysed in IP buffer [20 mM HEPES, pH 7.4, 100 mM NaCl, 2 mM $CaCl_2$, 1 mM $MgCl_2$, 1% Triton X-100, 1 mM PMSF, pepstatin (1 μg/mL), aprotinin (2 μg/mL), leupeptin (1 μg/mL)] and rotated for overnight at 4 °C. The lysate was spun for 15 min at 11,300 g and the supernatant was pre-cleared by incubating with washed Protein A with rotation for 1 h at 4 °C. The pre-cleared supernatant was incubated with the denoted antibody for 1 h at 4 °C and then with washed Protein A beads for 1.5 h at 4 °C. The beads were then washed five times with 1 mL of IP buffer, and the bound proteins were eluted by boiling 10 min in SDS-PAGE sample buffer.

2.10. Cell culture and transfection

HEK 293T cells were maintained in DMEM supplemented with 10% FBS and 1% penicillin/streptomycin and grown to 80% confluency in 25 cm^2 flasks. Cells were split into 6-well dishes and transfected using GenePORTER3000 lipid reagent, based on the provided protocol. Protein was harvested 48 h after transfection in homogenization buffer [(20 mM HEPES, pH 7.4, 100 mM NaCl, 1 mM PMSF, pepstatin (1 μg/mL), aprotinin (2 μg/mL), leupeptin (1 μg/mL), 1% Triton X-100)].

2.11. Statistics

All values are presented as the mean ± SEM, and $p < 0.05$ was considered statistically significant. Calculations were performed using the GraphPad Prism 4 software (San Diego, CA).

3. Results

3.1. Intrinsic oligomerization of CSPα mutants

We generated ANCL mutants by site-directed mutagenesis (Fig. 1) and characterized the biochemical properties of these proteins. As the ANCL mutations abolish palmitoylation of CSPα [14,16], we decided to explore the inherent properties of WT and mutant human CSPα proteins without lipid posttranslational modifications. WT and ANCL mutant CSPα proteins were overexpressed in BL21(DE3) *E. coli*, which like all bacterial strains lack the eukaryotic palmitoyltransferase enzymes needed to covalently attach palmitates to cysteine residues. Purified proteins (1 mg/mL) were subject to SDS-PAGE in the presence of 50 mM of DTT as previous studies have showed that oligomers of WT CSPα are SDS-resistant [18]. Coomassie staining and immunoblotting of purified proteins indicated that the protein purity exceeded 95% (Fig. 2A, D). The gels show that both L115R and L116Δ mutants exhibit noticeable oligomerization compared with the WT CSPα (Fig. 2A, B, D, E). Strikingly, oligomerization occurred even in the presence of 1000 fold molar excess reducing agent, suggesting that it is not due to the formation of disulfide bonds by the unpalmitoylated, free cysteines (Fig. 2A, D; Fig. S1). In the absence of DTT, both WT and mutant CSPα show a similar protein smear-like pattern as would be expected from non-specific disulfide bond formation (Fig. S1). The addition of DTT abolished the smear except for the specific oligomers seen in the case of ANCL mutants (Fig. S1).

Distinct oligomeric species were seen with the two ANCL mutants. The size of the oligomers for the L115R mutant were ~56, ~100 and ~250 kD, corresponding to dimer, tetramer and species with 8 or more monomers, while the size of the oligomer for the L116Δ mutant was ~250 kD (Fig. 2A, D). The dissimilar banding pattern suggests that the oligomerization behavior of L115R and L116Δ is different, but generates at least one common oligomeric ~250 kD species. As shown in Fig. 2E, the L115R mutant also produced higher molecular weight (HMW) oligomers (58.9 ± 5.9 fold versus WT) than the L116Δ mutant (13.2 ± 3.9 fold versus WT). In the case of L115R, oligomerization was

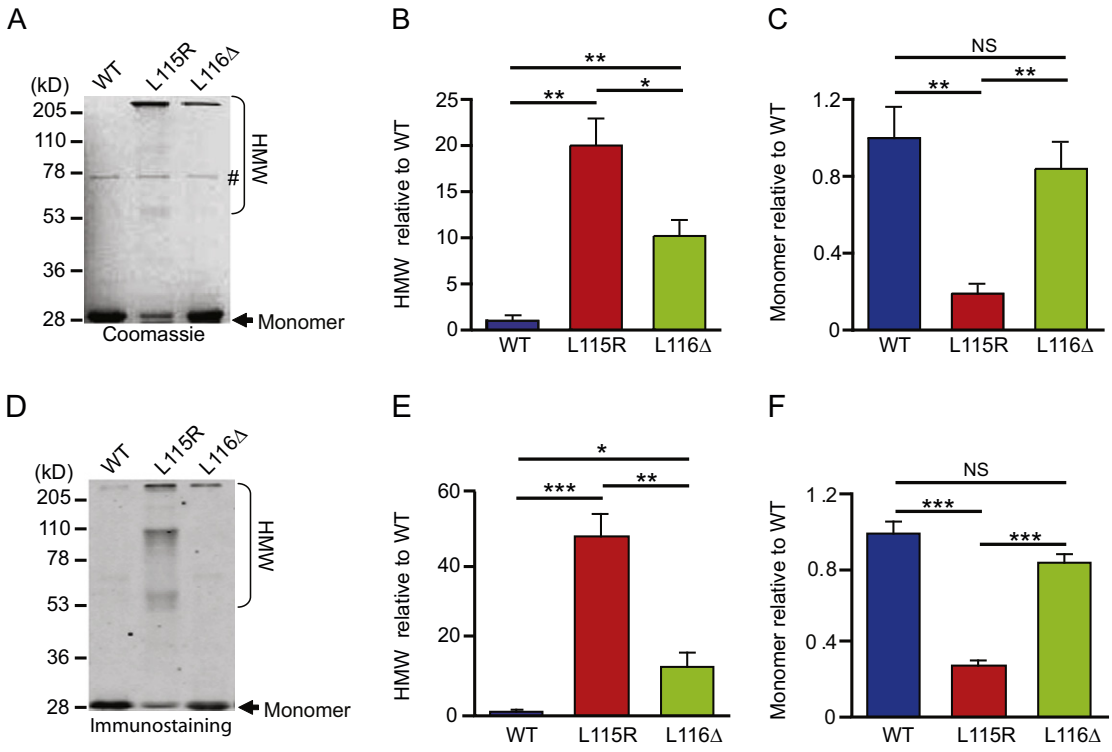

Fig. 2. Oligomerization of purified ANCL mutant CSPα proteins. (A) Coomassie staining of purified WT and mutant CSPα protein (5 μg). (B, C) Quantification of high molecular weight (HMW) oligomers and monomers shown in (A). (D) Immunoblotting of purified WT and mutant CSPα protein (1 μg). (E, F) Quantification of HMW oligomers and monomers shown in (D), respectively. The filled arrow indicates the monomer. #: contaminant band. The results are from three experiments and the quantification is expressed as average ± SEM. *$p < 0.05$; **$p < 0.01$; ***$p < 0.001$; NS: Not significant.

accompanied by an observable loss of monomeric protein (0.28 ± 0.03 fold versus WT; Fig. 2C and F). Taken together, both CSPα mutants are prone to oligomerize and form HMW oligomers which were DTT resistant, but the L115R mutant has the highest propensity to do so. Importantly, the oligomerization occurs in the absence of palmitoylation.

Given that both ANCL mutations are located in the proximity of cysteine string domain, we investigated whether the flanking domains, i.e. the J domain and C terminus (Fig. 1A; Fig. S2A), affect the oligomerization of CSPα mutants. We generated WT and mutant, J domain and C terminus deletions, and confirmed that we successfully deleted the relevant domains by staining with CSPα N terminus and C terminus epitope specific antibodies (Fig. S2C, D). As shown in Fig. S2, neither deletion of the J domain nor C terminus inhibits the oligomerization of the ANCL mutants (Fig. S2B, F). In fact, the deletion of the J-domain increased the abundance of oligomers for both WT and ANCL CSPα (Fig. S2B, D and E), indicating a possible inhibitory role. Overall, these data suggest that the cysteine string domain and the ANCL mutations are the key determinants of CSPα oligomerization. Our findings are consistent with the previously published results showing that amino acids 83–138 of WT CSPα, which include the cysteine string domain are important for self-assembly [18].

Next, we examined whether SGT, a clamp protein that stabilizes the CSPα/Hsc70 chaperone complex, played a significant role in oligomerization of ANCL mutants [7]. Surprisingly, SGT exhibited no effect on oligomerization of CSPα mutants (Fig. S3), and furthermore SGT was not observed to assemble into CSPα oligomers (Fig. S3A, B and D). These data suggest that oligomerization is an intrinsic protein property of ANCL mutant CSPα.

3.2. Characterization of oligomerization properties of mutant CSPα

For familiar neurodegenerative disease proteins such as Aβ and α-synuclein, it has been well established that increased protein concentration accelerates oligomerization and aggregation of mutant proteins [19,20]. To test whether CSPα behaved similarly, we prepared solutions of increasing protein concentrations (0.125–1.0 mg/mL; 5–40 μM) and subject them to SDS-PAGE and immunoblotting. Fig. 3A–C shows that raising protein concentration significantly augmented HMW oligomers and reduced monomer amounts for L115R. The three dominant species showed different concentration dependence with the ~100 and ~250 kD species exhibiting a significant increase with concentration (Fig. S4) while the ~56 kD did not, suggesting that the species >100 kD arise from monomers directly (Fig. S4). For the L116Δ mutant, we only observe the formation of the 250 kD species at a concentration of 1 mg/mL (Fig. 3A, B) and the monomer levels displayed a mild decrease compared with WT (Fig. 3C).

Another property for neurodegenerative associated proteins is their temperature dependence of oligomerization and aggregation [21]. Since the above western blots were performed after boiling the samples, two other temperatures, 37 °C and 69 °C, were chosen to treat the proteins prior to separation on SDS-PAGE. As seen in Fig. 3D–F, oligomeric intermediates were formed for L115R at all temperatures tested. Interestingly, WT and L116Δ form novel oligomeric species at 37 °C, several of which are shared with L115R, but these intermediates are abolished with the exception of the 250 kD species, upon increasing the temperature (Fig. 3D). Consistent with this, the monomer levels were increased as a function of temperature, reflecting an imbalance between the disassembly of non-specific oligomers and formation of mutant specific species (Fig. 3F and Fig. S1). The quantification of the CSPα band at 250 kD reveals that its levels increase with temperature for both mutants (Fig. 3E). The temperature dependence mirrors the concentration dependence of oligomer formation for the two ANCL mutants (Fig. 3B, E), again indicating different propensity to oligomerize.

To investigate this further, we varied the time of incubation at 37 °C. As shown in Fig. 3G–I, both mutants formed oligomers in a time-dependent manner, though the L116Δ has a longer lag. A noteworthy

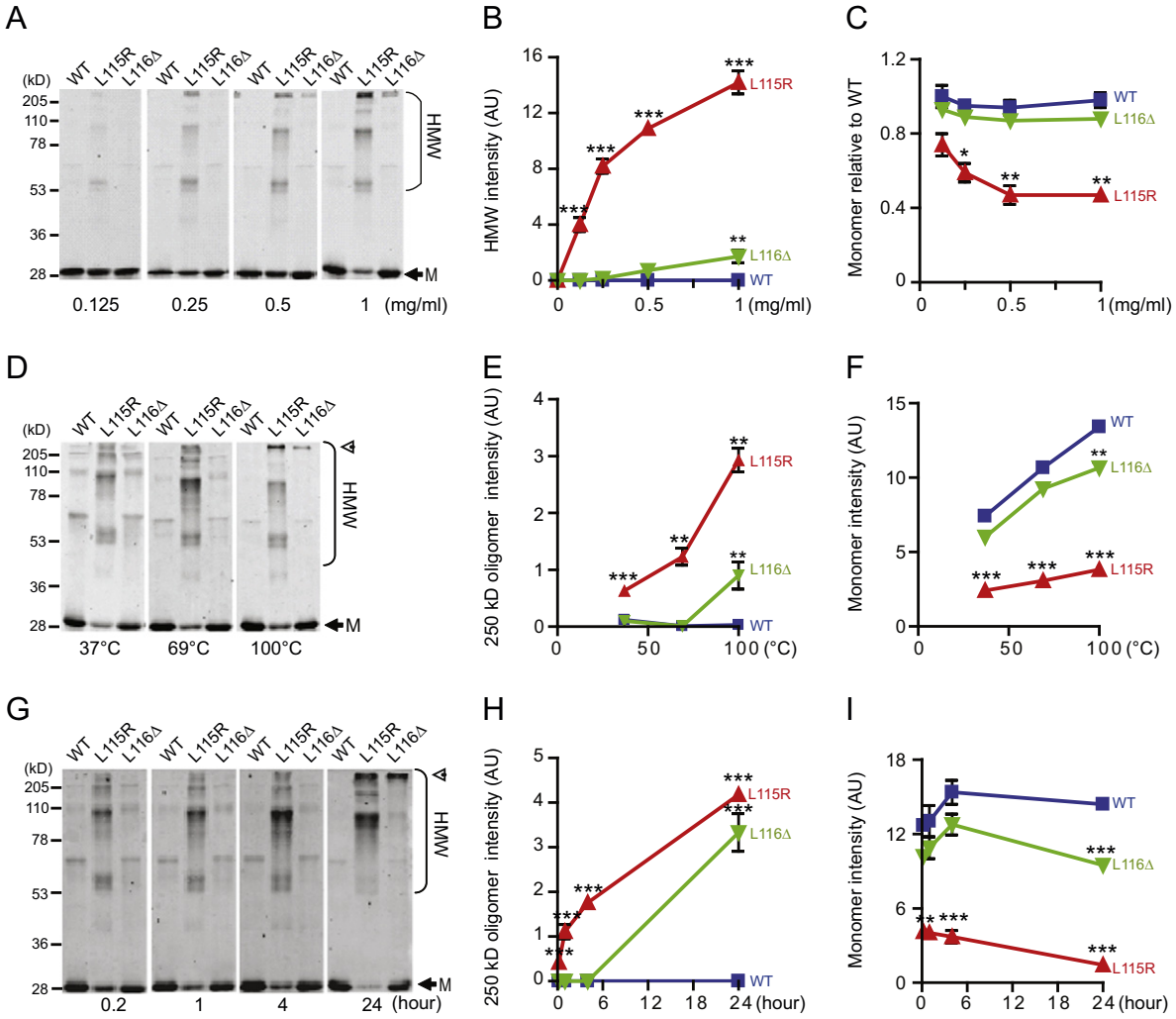

Fig. 3. Characterization of oligomerization of purified WT and mutant CSPα proteins. (A) Immunoblotting of increasing concentrations of purified WT and mutant CSPα proteins in the presence of 50 mM DTT. Blotting of 1 μg protein from solutions of 0.125, 0.25, 0.5, and 1 mg/mL is shown. (B, C) Quantification of HMW oligomers and monomers shown in (A), respectively. (D) Immunoblotting of 1 μg (concentration 1 mg/mL) of purified WT and mutant CSPα proteins with 50 mM DTT after heating at 37 °C, 69 °C and 100 °C for 10 min. (E, F) Quantification of the 250 kD oligomer and monomers is shown in (D), respectively. (G) Immunoblotting of 1 μg of 1 mg/mL of purified WT and mutant CSPα proteins incubated for 12 min, 1, 4, and 24 h at 37 °C. (H, I) Quantification of the 250 kD oligomer band and monomers is shown in (G), respectively. HMW: high molecular weight. The filled arrow indicates the monomer and the open arrowhead indicates 250 kD oligomer. All results are from at least three independent experiments. Statistical significance is denoted relative to WT. *$p < 0.05$; **$p < 0.01$; ***$p < 0.001$; NS: Not significant.

aspect is that the oligomer pattern obtained after incubating mutant proteins at 37 °C for 24 h mimics that at 100 °C for 10 min (Fig. 3G versus Fig. 2D). In these samples, the 250 kD species predominates indicating that this is a physiologically relevant species. We also did not observe macroscopic aggregates. In all, our data support the principle that oligomerization of CSPα mutants, like other neurodegenerative disease proteins, is concentration and time-dependent.

3.3. Co-chaperone function is impaired by oligomerization of CSPα mutants

CSPα functions as co-chaperone through its interactions with Hsc70 and its substrates [7,12]. We wanted to explore whether the ANCL mutations impact co-chaperone function of CSPα directly or indirectly through increased protein oligomerization. First, we determined the effect of ANCL mutations on freshly purified protein preparations which have equivalent amounts of monomeric proteins (Fig. 4A–D). We measured the ability of the CSPα mutants to accelerate the ATPase activity of Hsc70, via their J-domains. WT CSPα can readily accelerate the basal ATPase activity of Hsc70 by 2.5 fold consistent with the previously published results (Fig. 4A) [12,22]. As a negative control, we used a J-domain mutant (CSPα QPN) which has diminished Hsc70 binding and impaired ability to stimulate the ATPase activity of Hsc70 [12]. Remarkably, both the L115R and L116Δ mutants could robustly accelerate the ATPase activity of Hsc70 to the same level as WT protein (Fig. 4A, D). These enzymatic assay results indicate that the J-domain of the ANCL mutants can bind Hsc70 and is functional. Next, we examined the functionality of the C-terminal domain by assessing the ability of the ANCL mutants to bind specific CSPα clients. We tested binding to the two best characterized clients of CSPα—SNAP-25 and dynamin 1 [11, 12] by performing affinity chromatography using mouse brain homogenates. These experiments clearly demonstrate that the ANCL mutants can bind client proteins as effectively as WT CSPα (Fig. 4E). This biochemical interrogation revealed that ANCL CSPα mutants, when not oligomerized, are functional as co-chaperones. This is consistent with the fact that both ANCL mutations are in cysteine string domain and not in the J- or C-terminal domain.

To study the impact of oligomerization on CSPα co-chaperone activity, we incubated WT and ANCL mutant CSPα for 24 h at 37 °C, followed by Hsc70 ATPase assays. The L115R mutant's ability to stimulate Hsc70 ATPase activity was dramatically reduced by 80%, but no significant difference was observed for the L116Δ mutant compared with WT (Fig. 4F). The co-chaperone capacity of these protein preparations

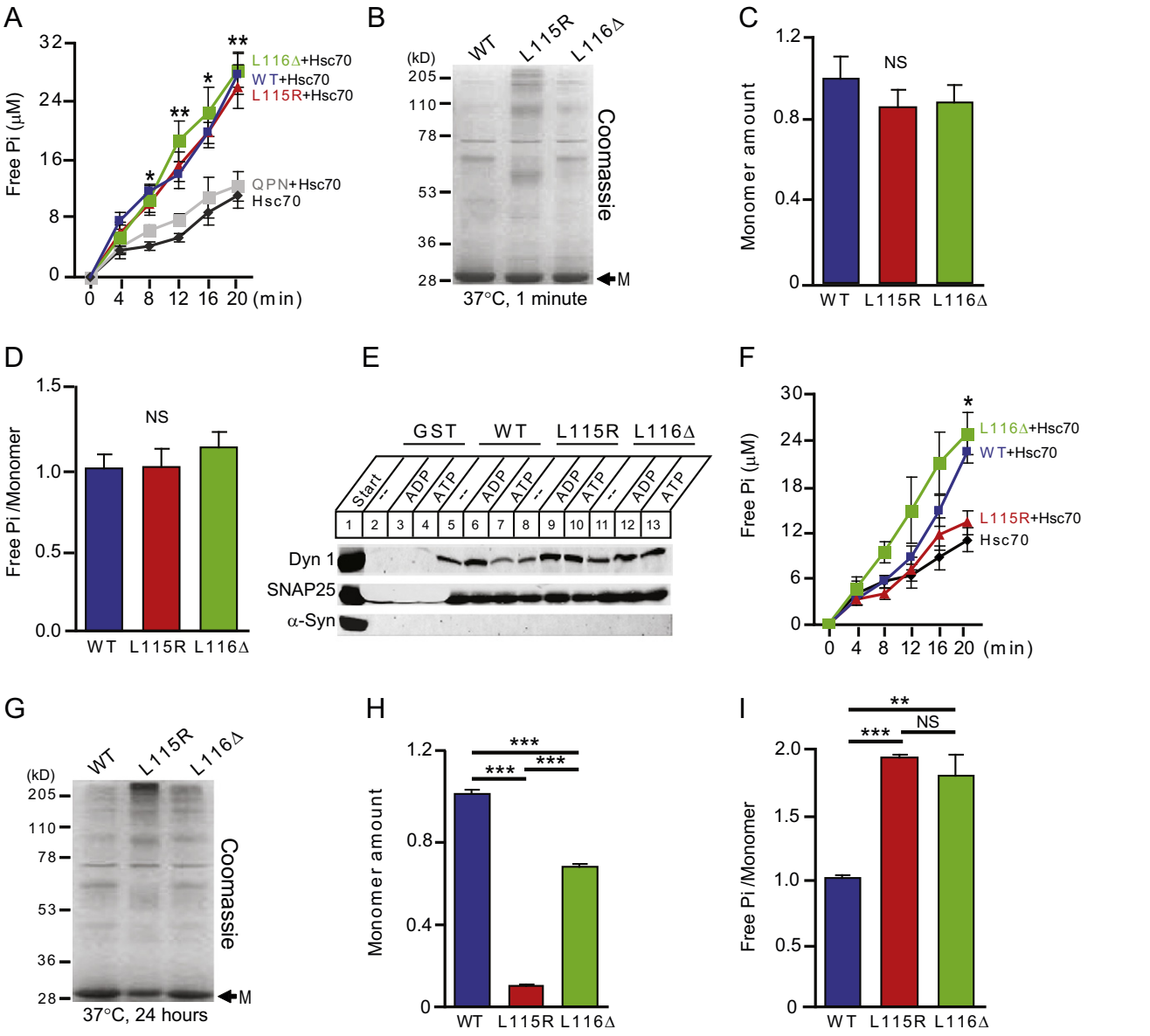

Fig. 4. Oligomerization of mutant CSPα proteins impacts co-chaperone activity. (A) ATPase assay using freshly purified WT and ANCL mutant CSPα. Statistical significance is relative to Hsc70 alone. (B, C) Coomassie staining of 5 μg freshly prepared WT and mutant CSPα used in (A) and quantification of monomer amount, respectively. (D) ATPase activity normalized to monomer amount, for data shown in (A). (E) Binding of substrates to ANCL mutants. Solubilized WT mouse brain homogenate (start) was incubated with GST (lanes 2–4), GST-CSPα WT (lanes 5–7), GST-CSPα L115R (lanes 8–10) and GST-CSPα L116Δ (lanes 11–13) beads in the absence of nucleotides (lanes 2, 5, 8, 11), or the presence of 5 mM ADP (lanes 3, 6, 9, 12) or ATP (lanes 4, 7, 10, 13), and bound proteins were analyzed by immunoblotting. WT and CSPα mutants bind known CSPα substrates dynamin 1 and SNAP-25 equally. α-Synuclein was used as a negative control. (F) ATPase assay using purified proteins after 24 h of incubation at 37 °C. Statistical significance is relative to Hsc70 alone. (G, H) Coomassie staining of incubated proteins (5 μg; 24 h) of WT and mutant CSPα used for ATPase assay in (F) and quantification of monomer amount, respectively. (I) ATPase activity normalized to monomer amount, for data shown in (F). All results are from at least three independent experiments. *$p < 0.05$; **$p < 0.01$; ***$p < 0.001$; NS: Not significant.

largely reflects the amount of monomer protein remaining, as only 10% of L115R but still 66% of L116Δ monomer was left after 24 h (Fig. 4G, H). Nonetheless, the decrease in monomer levels is more affected than enzymatic activity, and can be seen by normalizing ATPase activity to CSPα monomers amount (Fig. 4I). This implies that perhaps dimeric CSPα species retain ATPase stimulatory activity as suggested previously [17], while other HMW oligomers are not functional.

3.4. Co-oligomerization of WT and mutants attenuates co-chaperone activity of CSPα

ANCL occurs in the heterozygous state with one copy each of WT and mutant CSPα. To model the disease condition, we mixed WT and ANCL mutants in a 1:1 M ratio (0.5 mg/mL), and incubated the proteins for 24 h at 37 °C. We first examined the oligomeric profiles of the mixtures and compared it to the individual proteins. Intriguingly, both ANCL mutants when mixed with WT protein formed the 250 kDa species, even though both WT and L116Δ individually did not do so under these lower protein conditions (Fig. 5A). Quantifications confirmed that the WT:ANCL mixtures do indeed oligomerize to a greater extent (Fig. 5B) and are accompanied by a larger loss of monomer (Fig. 5C). Next, we used these mixtures to test their efficacy in the Hsc70 ATPase assays and compared them to the same proteins incubated alone. We observed that ATPase activity of the mixtures was significantly lower than what one would expect from the sum of the individual protein activity (Fig. 5D). This would suggest that the mixtures oligomerize to a greater extent and that hetero-oligomers of WT and ANCL mutants are not enzymatically active. It is important to note that both the L115R and L116Δ mutants behave similarly in the presence of WT protein, consistent with the similar phenotypes seen in patients.

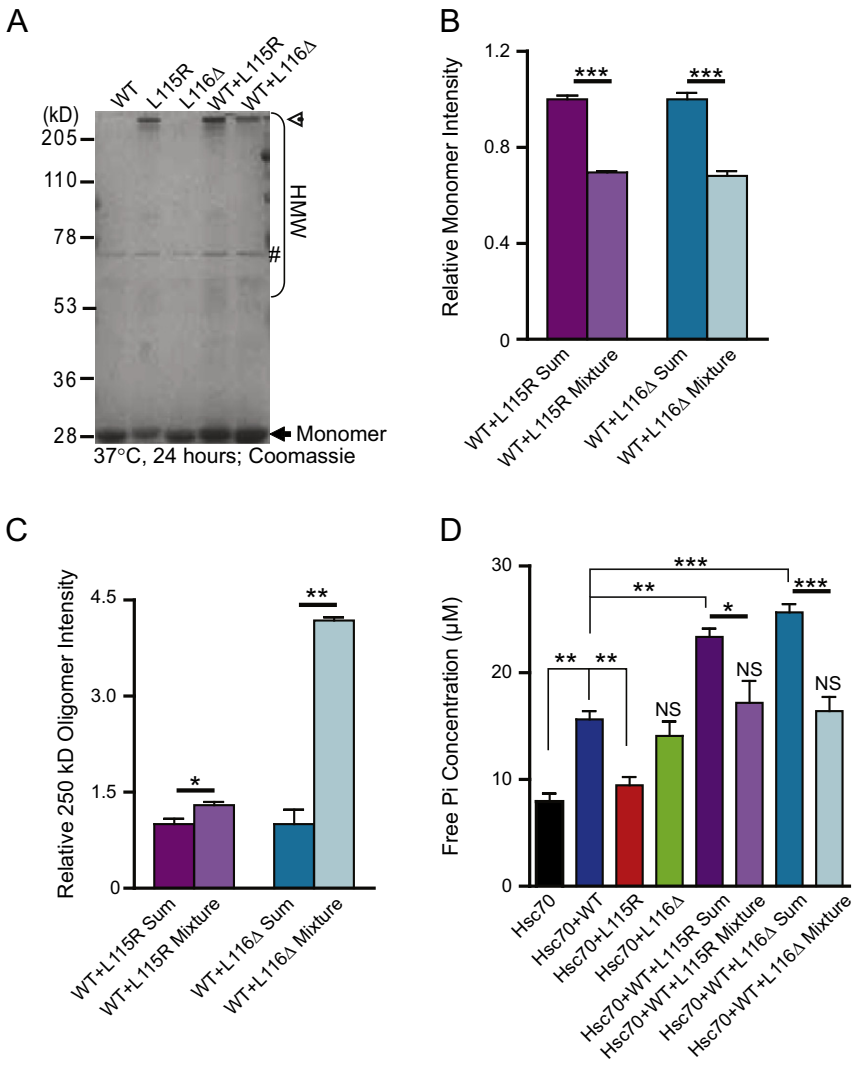

Fig. 5. Oligomerization of WT and ANCL mutant mixtures in vitro. (A) Coomassie staining of 2.5 μg of individual or 5 μg of mixture of WT CSPα and ANCL mutant. 0.5 mg/mL of WT CSPα and ANCL mutant was mixed by 1:1, followed by incubation for 24 h at 37 °C. Individual WT CSPα or ANCL mutant was used as controls. (B, C) Quantification of relative intensity of monomers (B) and 250 kD oligomers (C) in the mixture of WT CSPα and ANCL mutant. The actual values observed for the mixture were compared to the hypothetical sum of monomers or oligomers obtained with individual proteins after setting this value to '1'. (D) ATPase assay using individual or mixture of WT CSPα and ANCL mutant. The free phosphate concentration was measured at 20 min after incubation. The thick line indicates the comparison between individual sum and mixture, and the remaining denotations present statistical comparisons between individual WT and all other conditions. HMW: high molecular weight. The filled arrow indicates the monomer and the open arrowhead indicates 250 kD oligomer. #: contaminant band. All results are from at least three independent experiments.*$p < 0.05$; **$p < 0.01$; ***$p < 0.001$; NS Not significant.

3.5. Oligomerization of CSPα mutants in HEK 293T cells

Our experiments using purified proteins suggest that oligomerization is an intrinsic property of ANCL CSPα mutants. This raises the question whether this is purely an *in vitro* phenomenon or could also occur in mammalian cells. To examine this matter, WT and the ANCL proteins were overexpressed in HEK 293T cells. Cell lysates were incubated at 37 °C, separated on SDS-PAGE and blotted for CSPα (Fig. 6A–C). Both ANCL mutants exhibited observable oligomerization, (Fig. 6A), resembling the purified proteins in vitro (Fig. 1A, D). Consistent with the purified protein data (Fig. 2), all oligomeric intermediates shifted to the top of the gel when the samples were boiled (Fig. 6D–F).

In HEK 293T cells, the palmitoylation of monomers was severely impaired for the ANCL mutants (Fig. 6A, D; S5) in line with previous reports [16]. To test if the oligomers were palmitoylated, an aliquot of the same HEK 293T cell lysate was treated overnight at 4 °C with hydroxylamine (HA), a chemical that depalmitates proteins. A slight decrease in oligomers and increase of monomers were detected for the L115R (0.9 ± 0.016 fold of HMW/monomer versus 'No HA') and L116Δ mutants (0.95 ± 0.02 fold of HMW/monomer versus 'No HA') (Fig. 6F), with only a few selected bands disappearing upon hydroxylamine treatment, even though the WT monomeric CSPα was completely depalmitoylated under these conditions (Fig. 6A, D). This suggests that in HEK 293T cells, ANCL CSPα oligomers were largely not palmitoylated. Next, we tested if the soluble oligomers formed insoluble macroscopic aggregates, as seen in other dominantly inherited neurodegenerative diseases. Pellet fractions from transfected HEK 293T cells were subject to centrifugation steps to enrich for aggregates and solubilized in 8 M urea containing sample buffer. Neither monomer nor oligomer was present in the pellet (data not shown), suggesting no insoluble aggregates were formed. This finding is congruent with the lack of overt CSPα neuropathology in ANCL brains [14]. The similarity of oligomerization of CSPα mutants both *in vitro* and in mammalian cells indicates that CSPα oligomers are indeed newly gained species in ANCL.

3.6. Co-oligomerization of WT and mutants when co-expressed in HEK 293T cells

Our *in vitro* experiments using mixtures of WT and mutant CSPα protein demonstrated an overall increase in oligomerization and

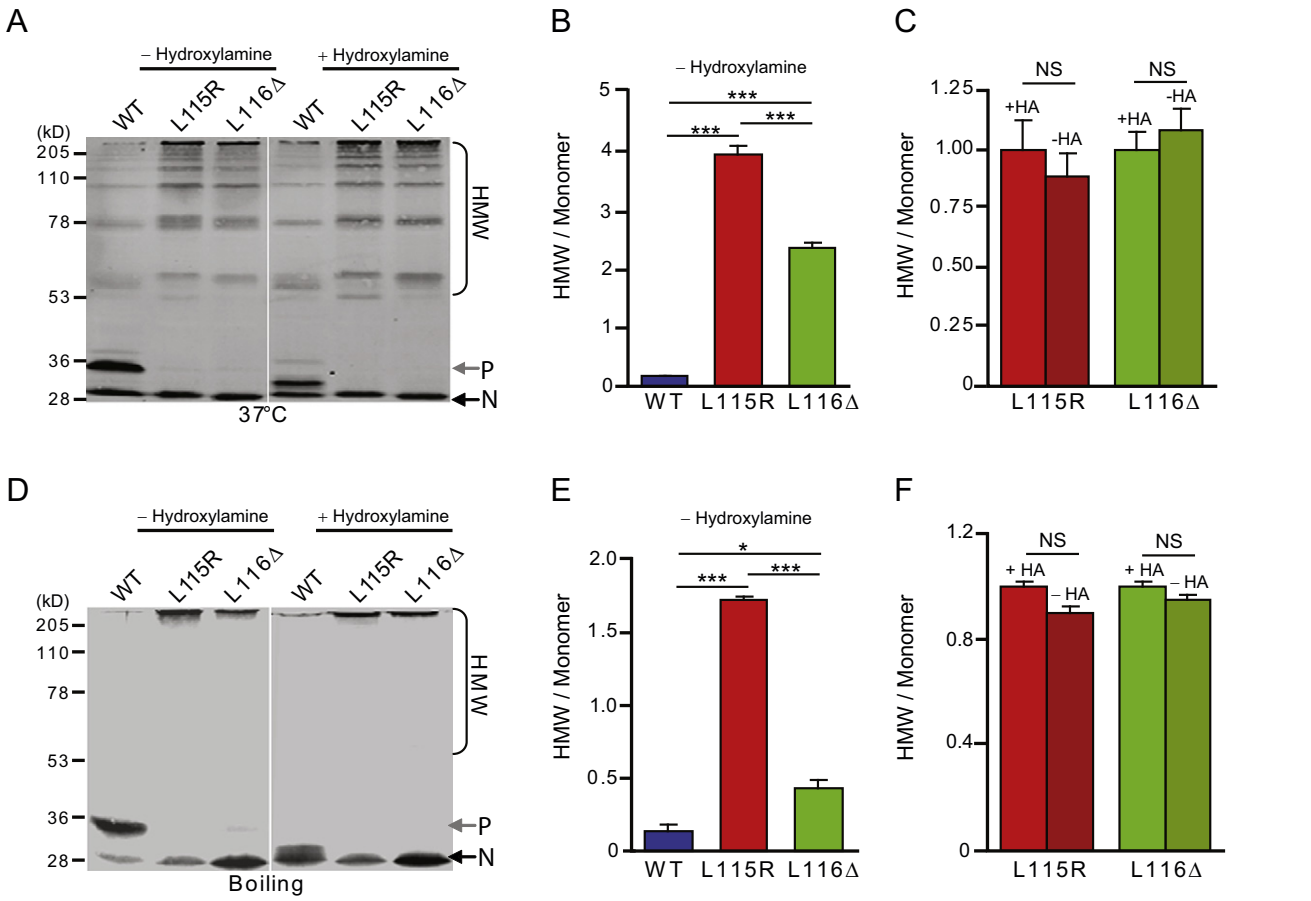

Fig. 6. Oligomerization of CSPα mutants in HEK 293T cells. (A) Immunoblotting of WT and mutant CSPα in supernatant fractions of HEK 293T cells. The samples were treated without or with hydroxylamine (HA; 1 M) overnight at 4 °C and heated at 37 °C for 10 min before subject to SDS-PAGE. (B) The ratio of HMW oligomers to monomers without HA treatment. (C) Comparison of the ratio of HMW oligomers to monomers with and without HA treatment for L115R and L116Δ at 4 °C. (D, E and F) Same as (A, B and C) except that the samples were boiled instead of heating at 37 °C. HMW: high molecular weight; P: palmitoylated monomer; N: non-palmitoylated monomer. All results are from at least three independent experiments.*$p < 0.05$; ***$p < 0.001$; NS: Not significant.

concomitant decrease in co-chaperone activity (Fig. 5). However, we cannot exclude that the oligomers are derived only from the mutant rather than from both WT and mutant. To test whether the ANCL mutant proteins are capable of forming mixed oligomers with the WT protein, we used FLAG and Myc tagged CSPα constructs and co-expressed them in HEK 293T cells. Western blotting with FLAG or Myc antibody confirmed that the tagged proteins behave similar to untagged versions, with the ANCL mutants forming 250 kD oligomers to a greater extent than WT CSPα (Fig. 7A, B, E, F versus Fig. 6D, E). The co-expression of Myc tagged WT with FLAG tagged mutant and vice versa significantly promoted the formation of WT oligomers (Fig. 7C, D, G, H), indicating the formation of mixed oligomers.

3.7. Ubiquitination of oligomers formed by both WT and mutant CSPα

The above HEK 293T experiments establish that the ANCL mutants are not palmitoylated and readily oligomerize compared to WT CSPα (Fig. 6). Based on these findings, we tested whether CSPα oligomers are selectively targeted for degradation. CSPα proteins were immunoprecipitated from HEK 293T cell lysates and probed with an antibody that recognizes poly-ubiquitination, a covalent modification that targets proteins for degradation. As shown in Fig. 8A, CSPα antibody could immunoprecipitate and enrich both monomers and oligomers. Fascinatingly, the poly-ubiquitin antibody only significantly recognized the 250 kD band whose signal intensity correlated with the amount of CSPα positive oligomers (Fig. 8B, C).

4. Discussion

4.1. Gain and loss of function mechanisms underlie ANCL

In this study, we systemically characterized the two ANCL causing mutants—L115R and L116Δ. Unlike other recessive NCL mutations which directly abrogate the normal function of the associated proteins, dominant CSPα mutations had no adverse effect on CSPα co-chaperone activity and substrates binding affinity, instead they drove the formation of novel oligomeric species which in turn disrupted the function of both WT and mutant CSPα. Here we propose that the oligomerization of CSPα mutants is a gain-of-function which directly leads to a loss-of-function based on several observations. 1) The oligomerization of ANCL CSPα mutants occurs extensively and in a time, concentration, and temperature dependent manner (Fig. 3). 2) The loss of co-chaperone activity of mutant CSPα depends on protein oligomerization. In the absence of oligomerization, WT and mutant stimulate ATPase activity of Hsc70 equivalently (Fig. 4A); indicating that the mutation itself does not affect the inherent function of CSPα. Further, the decrease in CSPα co-chaperone activity largely reflects the loss of monomers by oligomerization (Fig. 4F–H). 3) The co-oligomerization of WT and mutants occurs both *in vitro* and in mammalian cells (Figs. 5, 7). Thereby, co-oligomerization makes it feasible for one mutant *CLN4/DNAJC5* allele to result in the dysfunction of CSPα protein encoded by both alleles and most likely accounts for the dominant nature of ANCL. 4) In support of a loss-of-function mechanism, we observe mislocalization of both WT and mutant CSPα in the cell body away from synaptic

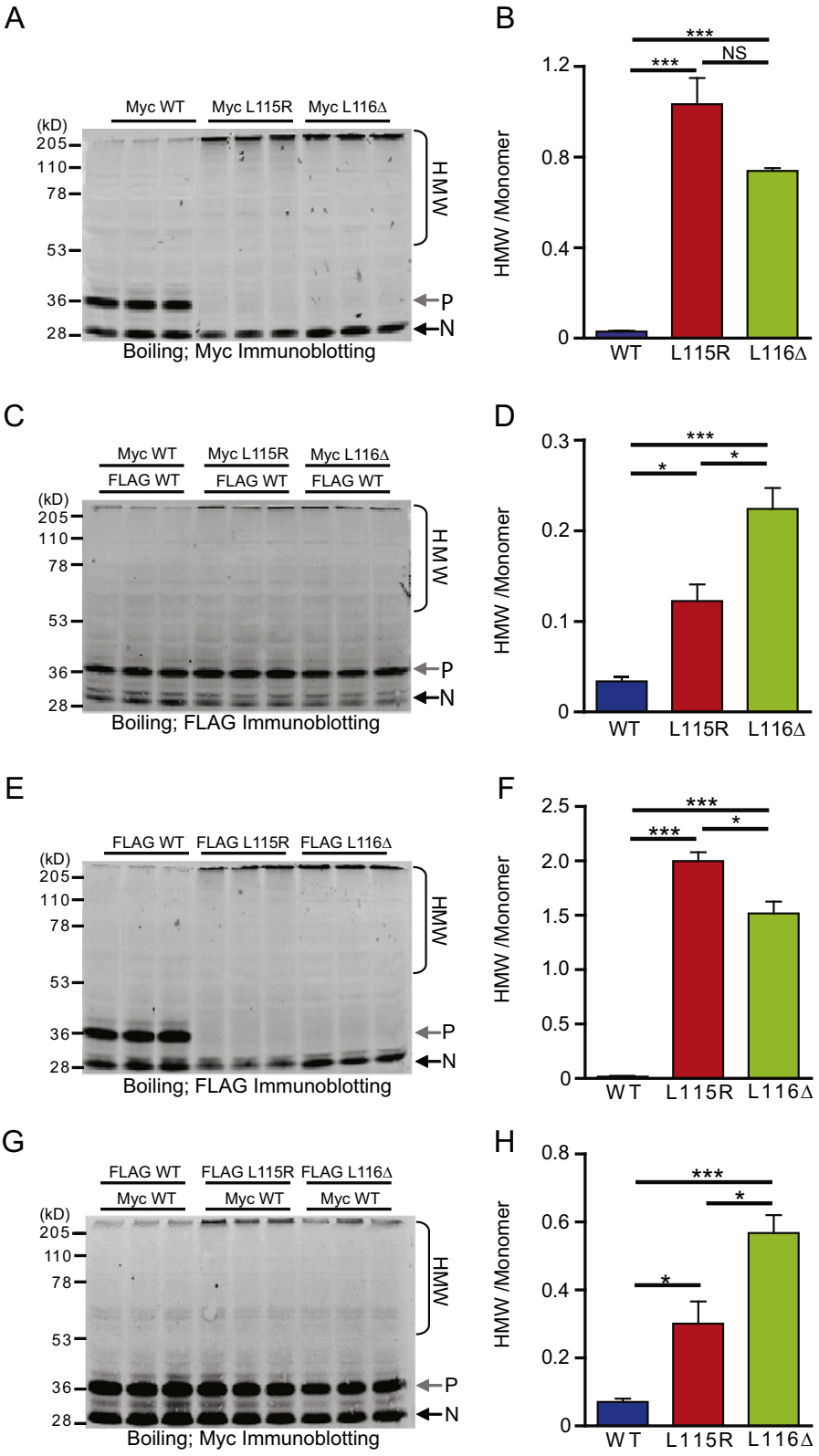

Fig. 7. Oligomerization WT and ANCL mutant mixtures in HEK 293T cells. (A, B) Immunoblotting of Myc-tagged WT and mutant CSPα overexpressed in HEK 293T cells and the quantification of the ratio of HMW oligomers to monomers. (C, D) The co-expression of FLAG-tagged WT CSPα with Myc-tagged WT or mutant CSPα and quantification of the ratio of HMW oligomers to monomers for FLAG-tagged WT CSPα. (E, F) Immunoblotting of FLAG-tagged WT and mutant CSPα overexpressed in HEK 293T cells and the quantification of the ratio of HMW oligomers to monomers. (G, H) Co-expression of Myc-tagged WT CSPα with FLAG-tagged WT or mutant CSPα and the quantification of the ratio of HMW oligomers to monomers for Myc-tagged WT CSPα. HMW: high molecular weight; P: palmitoylated monomer; N: non-palmitoylated monomer. All results are from at least three independent experiments. *$p < 0.05$; **$p < 0.01$; ***$p < 0.001$; NS: Not significant.

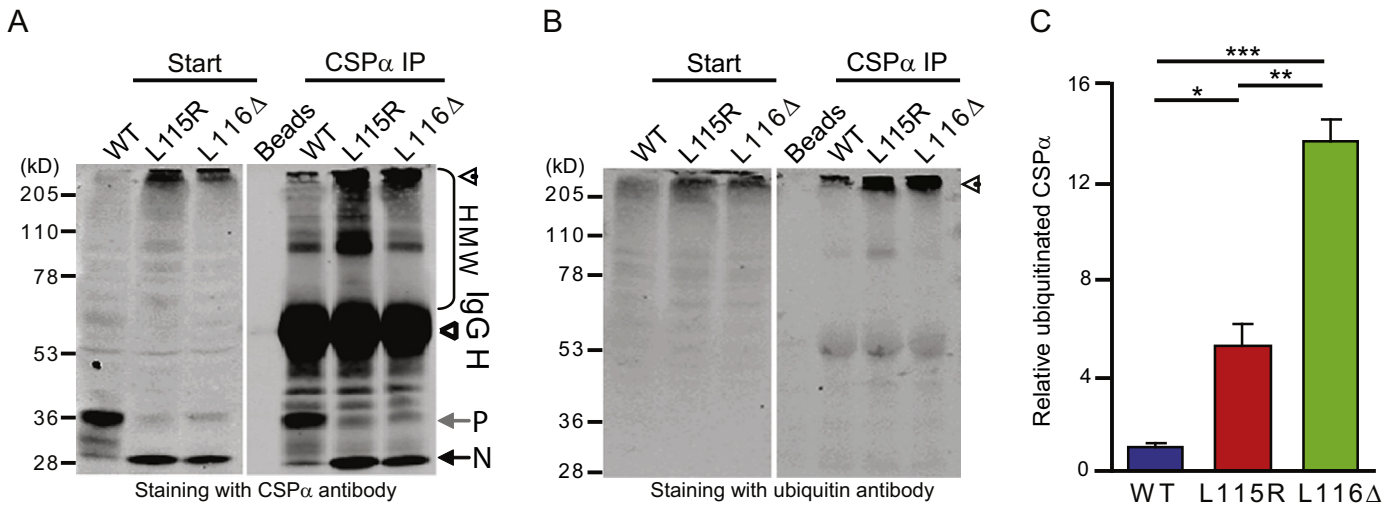

Fig. 8. Ubiquitination of oligomers of CSPα mutants in HEK 293T cells. (A, B) Immunoprecipitation of CSPα from HEK 293T cell lysates overexpressing WT and mutant CSPα, and immunoblotting for CSPα (A) and ubiquitin (B). (C) Quantification of ubiquitinated CSPα oligomers, for data shown in (B). HMW: high molecular weight; P: palmitoylated monomer; N: non-palmitoylated monomer. All results are from at least three independent experiments.*$p < 0.05$; **$p < 0.01$; ***$p < 0.001$.

termini in neurons (Henderson et al., Manuscript in preparation). These findings point to ANCL operating in a dominant negative manner.

While oligomerization is a common molecular feature of autosomal-dominant inherited neurodegenerative diseases—such as Alzheimer's disease, Parkinson's disease, and ALS—for these diseases oligomerization does not appear to result in a loss-of-function. This is supported by the fact that the deletion of the corresponding disease causing genes—APP, α-synuclein and superoxide dismutase 1—from mice genome results in no or subtle phenotype [23–25], unlike patients or transgenic mice that overexpress mutant proteins [26–28]. One dominant neurodegenerative disease clearly shown to be caused by both a gain and partial loss-of-function is spinocerebellar ataxia 1 [29]. Mutations in ataxin 1 cause spinocerebellar ataxia 1, but do not involve protein oligomerization. In marked contrast to these neurodegenerative diseases, in ANCL, an oligomerization dependent loss-of function is likely to underlie its pathogenesis as CSPα knockout mice phenocopy ANCL patients. CSPα knockout mice show progressive neurodegeneration and exhibit phenotypes such as seizures, motor deficits, and premature death seen in patients. Our data adds to growing evidence that for dominantly inherited neurodegenerative diseases, multiple mechanisms of action are likely to underlie disease pathophysiology.

Though we have clearly demonstrated an oligomerization-dependent loss of CSPα co-chaperone activity, it remains possible that the oligomers have additional modes of action. CSPα is a synaptic vesicle associated protein which is synthesized in endoplasmic reticulum (ER), transported to synaptic terminal via the Golgi and degraded in lysosomes [30]. Considering the stringent protein quality control that occurs at the ER, a question that remains to be addressed is whether oligomerization of CSPα mutants also causes ER stress and subsequently the unfolded protein response [31,32]. Similarly, possible deleterious effect of oligomers on Golgi and lysosomes needs more investigation. However, these studies are beyond the scope of the present work.

4.2. Distinct oligomerization pathways for L115R and L116Δ mutants

Although the L115R and L116Δ mutations are localized to cysteine string domain and even are next to each other, previous *in silico* analysis had predicted dissimilar alterations on biophysical and biochemical properties of CSPα. In keeping with this, we see clear differences in the oligomerization behavior for the L115R and L116Δ mutants both in terms of magnitude and time dependence. The L115R mutant was predicted to have a weaker membrane affinity which possibly facilitates self-assembly. Consistent with this prediction, we demonstrate that L115R is more potent to oligomerize than L116Δ. Interestingly, L115R patient brains have been shown to have less CSPα protein levels compared to L116Δ brains [14]. The two mutants also differ in the dynamic pattern of oligomerization. The L116Δ mutant resembles the WT oligomer pattern but with a higher abundance, in contrast, the L115R oligomer pattern clearly varies from WT and L116Δ (Fig. 3D, G; Fig. 4B, G; Fig. S2B; Fig. S3C). Yet, both mutants generate at least one common 250 kDa oligomeric species, strongly suggesting that this may be a disease relevant oligomer.

Interestingly, the co-oligomerization of L115R and L116Δ with WT is very similar, in spite of the different potentials for self-assembly. As a consequence, L116Δ appears to be more potent than L115R to co-oligomerize with WT CSPα. On the other hand, L115R oligomerization stands out with respect to its ability to self-assemble. Hence, we predict that ANCL patients carrying different mutants might show subtle differences in age of onset, speed of progress and duration of disease.

4.3. Post-translational modifications on ANCL mutants

Both ANCL mutations abolish palmitoylation of monomeric CSPα in HEK 293T cells. This is most likely because the leucines mutated in ANCL are needed to target CSPα to the membrane allowing the palmitoylacyltransferases to palmitoylate CSPα [33]. Our findings on the impact of ANCL mutations on palmitoylation are congruent with those reported by Greaves et al. [16]. However, in contrast to the reported work, we do not find any effect of palmitoylation on protein oligomerization. This may be due to the fact that palmitoylacyltransferases were overexpressed to make this point [16]. The fact that recombinantly produced protein from *E. coli* which lack palmitoylation also aggregates strongly support our case that palmitoylation is not required for ANCL mutant oligomerization. In contrast to a role for palmitoylation, we observed that the 250 kD oligomer is selectively ubiquitinated. It is widely accepted that ubiquitination can serve as a signal for degradation of lysosomes [34]. Hence, we hypothesize that the degradation of CSPα oligomers via lysosomes over time leads to lysosomal dysfunction and lipofuscin deposition.

5. Conclusion

Here we provide the evidence that ANCL mutants, CSPα L115R and L116Δ, could undergo self-oligomerization and co-oligomerization with WT CSPα. Oligomerization is therefore a gain-of-function as result of these mutations, but leads to a loss of co-chaperone activity of CSPα.

Hence, we propose a mechanism involving both a gain-of-function and a loss-of-function of CSPα causes ANCL. Our findings are congruent with the fact that ANCL is a dominant disease and helps explain the phenotypes seen in *CLN4* patients. Altogether, our data highlight the role of protein oligomerization in ANCL and suggest that disrupting oligomerization of CSPα mutants may be an effective therapy for treating ANCL.

Conflict of interests

The authors declare no conflict of interest.

Acknowledgments

We would like to thank the members of our laboratories for critical discussions related to this paper. This work was supported by the Battens Disease Research and Support Association Grant, the NIH R01NS083846, the NIH R01NS064963, and the NIDA Neuroproteomic Center Grant (5 P30 DA018343-07).

Appendix A. Supplementary data

Supplementary data to this article can be found online at http://dx.doi.org/10.1016/j.bbadis.2014.07.009.

References

[1] A. Jalanko, T. Braulke, Neuronal ceroid lipofuscinoses, Biochim. Biophys. Acta 1793 (2009) 697–709.
[2] A. Kyttala, U. Lahtinen, T. Braulke, S.L. Hofmann, Functional biology of the neuronal ceroid lipofuscinoses (NCL) proteins, Biochim. Biophys. Acta 1762 (2006) 920–933.
[3] S.E. Mole, R.E. Williams, H.H. Goebel, Correlations between genotype, ultrastructural morphology and clinical phenotype in the neuronal ceroid lipofuscinoses, Neurogenetics 6 (2005) 107–126.
[4] M. Kousi, A.E. Lehesjoki, S.E. Mole, Update of the mutation spectrum and clinical correlations of over 360 mutations in eight genes that underlie the neuronal ceroid lipofuscinoses, Hum. Mutat. 33 (2011) 42–63.
[5] D.N. Palmer, L.A. Barry, J. Tyynela, J.D. Cooper, NCL disease mechanisms, Biochim. Biophys. Acta 1832 (2013) 1882–1893.
[6] N. Zhong, Neuronal ceroid lipofuscinoses and possible pathogenic mechanism, Mol. Genet. Metab. 71 (2000) 195–206.
[7] S. Tobaben, P. Thakur, R. Fernandez-Chacon, T.C. Sudhof, J. Rettig, B. Stahl, A trimeric protein complex functions as a synaptic chaperone machine, Neuron 31 (2001) 987–999.
[8] S. Chandra, G. Gallardo, R. Fernandez-Chacon, O.M. Schluter, T.C. Sudhof, Alpha-synuclein cooperates with CSPalpha in preventing neurodegeneration, Cell 123 (2005) 383–396.
[9] R. Fernandez-Chacon, M. Wolfel, H. Nishimune, L. Tabares, F. Schmitz, M. Castellano-Munoz, C. Rosenmund, M.L. Montesinos, J.R. Sanes, R. Schneggenburger, T.C. Sudhof, The synaptic vesicle protein CSP alpha prevents presynaptic degeneration, Neuron 42 (2004) 237–251.
[10] J.L. Rozas, L. Gomez-Sanchez, J. Mircheski, P. Linares-Clemente, J.L. Nieto-Gonzalez, M.E. Vazquez, R. Lujan, R. Fernandez-Chacon, Motorneurons require cysteine string protein-alpha to maintain the readily releasable vesicular pool and synaptic vesicle recycling, Neuron 74 (2012) 151–165.
[11] M. Sharma, J. Burre, P. Bronk, Y. Zhang, W. Xu, T.C. Sudhof, CSPalpha knockout causes neurodegeneration by impairing SNAP-25 function, EMBO J. 31 (2011) 829–841.
[12] Y.Q. Zhang, M.X. Henderson, C.M. Colangelo, S.D. Ginsberg, C. Bruce, T. Wu, S.S. Chandra, Identification of CSPalpha clients reveals a role in dynamin 1 regulation, Neuron 74 (2012) 136–150.
[13] B.A. Benitez, D. Alvarado, Y. Cai, K. Mayo, S. Chakraverty, J. Norton, J.C. Morris, M.S. Sands, A. Goate, C. Cruchaga, Exome-sequencing confirms DNAJC5 mutations as cause of adult neuronal ceroid-lipofuscinosis, PLoS One 6 (2011) e26741.
[14] L. Noskova, V. Stranecky, H. Hartmannova, A. Pristoupilova, V. Baresova, R. Ivanek, H. Hulkova, H. Jahnova, J. van der Zee, J.F. Staropoli, K.B. Sims, J. Tyynela, C. Van Broeckhoven, P.C. Nijssen, S.E. Mole, M. Elleder, S. Kmoch, Mutations in DNAJC5, encoding cysteine-string protein alpha, cause autosomal-dominant adult-onset neuronal ceroid lipofuscinosis, Am. J. Hum. Genet. 89 (2011) 241–252.
[15] M. Velinov, N. Dolzhanskaya, M. Gonzalez, E. Powell, I. Konidari, W. Hulme, J.F. Staropoli, W. Xin, G.Y. Wen, R. Barone, S.H. Coppel, K. Sims, W.T. Brown, S. Zuchner, Mutations in the gene DNAJC5 cause autosomal dominant Kufs disease in a proportion of cases: study of the Parry family and 8 other families, PLoS One 7 (2012) e29729.
[16] J. Greaves, K. Lemonidis, O.A. Gorleku, C. Cruchaga, C. Grefen, L.H. Chamberlain, Palmitoylation-induced aggregation of cysteine-string protein mutants that cause neuronal ceroid lipofuscinosis, J. Biol. Chem. 287 (2012) 37330–37339.
[17] L.H. Chamberlain, R.D. Burgoyne, Activation of the ATPase activity of heat-shock proteins Hsc70/Hsp70 by cysteine-string protein, Biochem. J. 322 (Pt 3) (1997) 853–858.
[18] L.A. Swayne, C. Blattler, J.G. Kay, J.E. Braun, Oligomerization characteristics of cysteine string protein, Biochem. Biophys. Res. Commun. 300 (2003) 921–926.
[19] O.M. El-Agnaf, D.S. Mahil, B.P. Patel, B.M. Austen, Oligomerization and toxicity of beta-amyloid-42 implicated in Alzheimer's disease, Biochem. Biophys. Res. Commun. 273 (2000) 1003–1007.
[20] L. Breydo, J.W. Wu, V.N. Uversky, Alpha-synuclein misfolding and Parkinson's disease, Biochim. Biophys. Acta 1822 (2011) 261–285.
[21] K. Garai, C. Frieden, Quantitative analysis of the time course of Abeta oligomerization and subsequent growth steps using tetramethylrhodamine-labeled Abeta, Proc. Natl. Acad. Sci. U. S. A. 110 (2013) 3321–3326.
[22] J.E. Braun, S.M. Wilbanks, R.H. Scheller, The cysteine string secretory vesicle protein activates Hsc70 ATPase, J. Biol. Chem. 271 (1996) 25989–25993.
[23] H. Zheng, M. Jiang, M.E. Trumbauer, D.J. Sirinathsinghji, R. Hopkins, D.W. Smith, R.P. Heavens, G.R. Dawson, S. Boyce, M.W. Conner, K.A. Stevens, H.H. Slunt, S.S. Sisoda, H. Y. Chen, L.H. Van der Ploeg, beta-Amyloid precursor protein-deficient mice show reactive gliosis and decreased locomotor activity, Cell 81 (1995) 525–531.
[24] A.G. Reaume, J.L. Elliott, E.K. Hoffman, N.W. Kowall, R.J. Ferrante, D.F. Siwek, H.M. Wilcox, D.G. Flood, M.F. Beal, R.H. Brown Jr., R.W. Scott, W.D. Snider, Motor neurons in Cu/Zn superoxide dismutase-deficient mice develop normally but exhibit enhanced cell death after axonal injury, Nat. Genet. 13 (1996) 43–47.
[25] A. Abeliovich, Y. Schmitz, I. Farinas, D. Choi-Lundberg, W.H. Ho, P.E. Castillo, N. Shinsky, J.M. Verdugo, M. Armanini, A. Ryan, M. Hynes, H. Phillips, D. Sulzer, A. Rosenthal, Mice lacking alpha-synuclein display functional deficits in the nigrostriatal dopamine system, Neuron 25 (2000) 239–252.
[26] M.K. Lee, W. Stirling, Y. Xu, X. Xu, D. Qui, A.S. Mandir, T.M. Dawson, N.G. Copeland, N. A. Jenkins, D.L. Price, Human alpha-synuclein-harboring familial Parkinson's disease-linked Ala-53 → Thr mutation causes neurodegenerative disease with alpha-synuclein aggregation in transgenic mice, Proc. Natl. Acad. Sci. U. S. A. 99 (2002) 8968–8973.
[27] C.M. Karch, M. Prudencio, D.D. Winkler, P.J. Hart, D.R. Borchelt, Role of mutant SOD1 disulfide oxidation and aggregation in the pathogenesis of familial ALS, Proc. Natl. Acad. Sci. U. S. A. 106 (2009) 7774–7779.
[28] D. Games, D. Adams, R. Alessandrini, R. Barbour, P. Berthelette, C. Blackwell, T. Carr, J. Clemens, T. Donaldson, F. Gillespie, et al., Alzheimer-type neuropathology in transgenic mice overexpressing V717F beta-amyloid precursor protein, Nature 373 (1995) 523–527.
[29] J. Lim, J. Crespo-Barreto, P. Jafar-Nejad, A.B. Bowman, R. Richman, D.E. Hill, H.T. Orr, H.Y. Zoghbi, Opposing effects of polyglutamine expansion on native protein complexes contribute to SCA1, Nature 452 (2008) 713–718.
[30] J. Greaves, C. Salaun, Y. Fukata, M. Fukata, L.H. Chamberlain, Palmitoylation and membrane interactions of the neuroprotective chaperone cysteine-string protein, J. Biol. Chem. 283 (2008) 25014–25026.
[31] B.D. Roussel, A.J. Kruppa, E. Miranda, D.C. Crowther, D.A. Lomas, S.J. Marciniak, Endoplasmic reticulum dysfunction in neurological disease, Lancet Neurol. 12 (2013) 105–118.
[32] P. Walter, D. Ron, The unfolded protein response: from stress pathway to homeostatic regulation, Science 334 (2011) 1081–1086.
[33] J. Greaves, L.H. Chamberlain, Dual role of the cysteine-string domain in membrane binding and palmitoylation-dependent sorting of the molecular chaperone cysteine-string protein, Mol. Biol. Cell 17 (2006) 4748–4759.
[34] S. Engelender, Ubiquitination of alpha-synuclein and autophagy in Parkinson's disease, Autophagy 4 (2008) 372–374.